



## Stabilization of PFAS-contaminated soil with sewage sludge- and wood-based biochar sorbents

Erlend Sørmo<sup>a,b,1</sup>, Clara Benedikte Mader Lade<sup>a,b,1,2</sup>, Junjie Zhang<sup>c</sup>, Alexandros G. Asimakopoulos<sup>c</sup>, Geir Wold Åsli<sup>a</sup>, Michel Hubert<sup>a</sup>, Aleksandar I. Goranov<sup>d</sup>, Hans Peter H. Arp<sup>a,c</sup>, Gerard Cornelissen<sup>a,b,\*</sup>

<sup>a</sup> Norwegian Geotechnical Institute (NGI), 0484 Oslo, Norway

<sup>b</sup> Faculty of Environmental Sciences and Natural Resource Management, Norwegian University of Life Sciences (NMBU), 1430 Ås, Norway

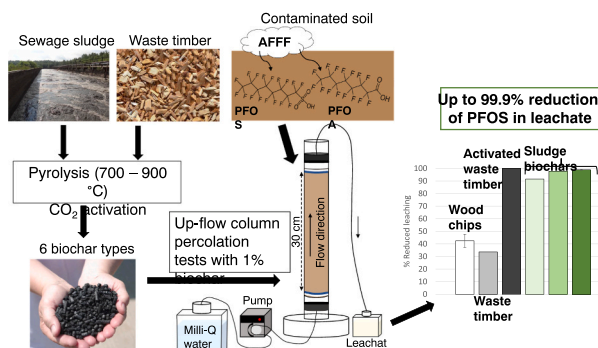
<sup>c</sup> Department of Chemistry, Norwegian University of Science and Technology (NTNU), 7024 Trondheim, Norway

<sup>d</sup> Department of Chemistry and Biochemistry, Old Dominion University, Norfolk, VA, USA

### HIGHLIGHTS

- Waste-based biochars were applied to field-PFAS-contaminated soil in column tests.
- 1 % biochar doses were sufficient to reduce PFOS leaching rates by >90 %.
- Activated wood- and sewage sludge biochars were the most effective at reducing leaching.
- Sorption was weakened by the presence of diverse PFAS.

### GRAPHICAL ABSTRACT



### ARTICLE INFO

Editor: Jay Gan

#### Keywords:

PFAS  
Waste-based biochar  
Sorbents  
Column tests  
Soil stabilization

### ABSTRACT

Sustainable and effective remediation technologies for the treatment of soil contaminated with per- and polyfluoroalkyl substances (PFAS) are greatly needed. This study investigated the effects of waste-based biochars on the leaching of PFAS from a sandy soil with a low total organic carbon content (TOC) of  $0.57 \pm 0.04$  % impacted by PFAS from aqueous film forming foam (AFFF) dispersed at a former fire-fighting facility. Six different biochars (pyrolyzed at 700–900 °C) were tested, made from clean wood chips (CWC), waste timber (WT), activated waste timber (aWT), two digested sewage sludges (DSS-1 and DSS-2) and de-watered raw sewage sludge (DWSS). Up-flow column percolation tests (15 days and 16 pore volume replacements) with 1 % biochar indicated that the dominant congener in the soil, perfluorooctane sulphonic acid (PFOS) was retained best by the aWT biochar with a 99.9 % reduction in the leachate concentration, followed by sludge-based DWSS (98.9 %) and DSS-2 and DSS-1 (97.8 % and 91.6 %, respectively). The non-activated wood-based biochars (CWC and WT) on the other hand, reduced leaching by <42.4 %. Extrapolating this to field conditions, 90 % leaching of PFOS would occur after 15

\* Corresponding author at: Norwegian Geotechnical Institute (NGI), 0484 Oslo, Norway.

E-mail address: [gerard.cornelissen@ngi.no](mailto:gerard.cornelissen@ngi.no) (G. Cornelissen).

<sup>1</sup> Equal contributions.

<sup>2</sup> Present address: SWECO, Oslo, Norway.

<https://doi.org/10.1016/j.scitotenv.2024.170971>

Received 26 November 2023; Received in revised form 12 February 2024; Accepted 12 February 2024

Available online 24 February 2024

0048-9697/© 2024 The Authors. Published by Elsevier B.V. This is an open access article under the CC BY license (<http://creativecommons.org/licenses/by/4.0/>).

y for unamended soil, and after 1200 y and 12,000 y, respectively, for soil amended with 1 % DWSS-amended and aWT biochar. The high effectiveness of aWT and the three sludge-based biochars in reducing PFAS leaching from the soil was attributed largely to high porosity in a pore size range (>1.5 nm) that can accommodate the large PFAS molecules (>1.02–2.20 nm) combined with a high affinity to the biochar matrix. Other factors like anionic exchange capacity could play a contributing role. Sorbent effectiveness was better for long-chain than for short-chain PFAS, due to weaker, apolar interactions between the biochar and the latter's shorter hydrophobic CF<sub>2</sub>-tails. The findings were the first to demonstrate that locally sourced activated wood-waste biochars and non-activated sewage sludge biochars could be suitable sorbents for the ex situ stabilization and in situ remediation of PFAS-contaminated soil, bringing this technology one step closer to full-scale field testing.

## 1. Introduction

Per- and polyfluoroalkyl substances (PFAS) form a large group of synthetic fluorinated organic chemicals, which are known to be persistent in the environment due to their very strong and stable carbon-fluorine bonds. Many PFAS can also be highly mobile and/or bioaccumulative (Buck et al., 2011; Kissa, 2001; Krafft and Riess, 2015). These substances have been extensively used for decades in consumer products and industrial applications, resulting in their spread to the environment, and subsequent risk for exposure to humans that can result in severe health effects, such as endocrine disruption and carcinogenicity (Fenton et al., 2021; Zahm et al., 2023). The surfactant properties and their thermal stability of certain PFAS, such as perfluorosulfonic acids (PFSAs), fluorotelomer sulfonates (FTS) and perfluorocarboxylic acids (PFCAs) have made them ideal for use in firefighting foams such as aqueous film forming foam (AFFF) (Høisæter and Breedveld, 2022). Investigations of fire training facilities in Norway have shown contamination with PFAS from AFFF in both soil, groundwater, and surface waters at several airports, including Oslo airport at Gardermoen (Høisæter and Breedveld, 2022; Høisæter et al., 2019), as well as several similar sites around the world (Cordner et al., 2021; Ruyle et al., 2023). It is thus important to regulate the production and use of PFAS, as well as to remediate and limit the spread from already existing contaminated sites. PFAS contamination is expected to have a sustained impact on surrounding bodies of water for centuries if not remediated (Ruyle et al., 2023).

Today, a wide selection of options exists for remediation of soil contamination, such as biological degradation, (catalyzed) chemical oxidation, stabilization, soil washing and thermal treatment processes (Quinnan et al., 2022; Ross et al., 2018; Travar et al., 2020). However, many of these treatments only have limited effect, due to the recalcitrance and behaviour of PFAS in the environment. Short-chain PFAS are more difficult to remediate with conventional technologies due to their high mobility, compared to long-chain, more hydrophobic PFAS, resulting in short-chain PFAS more readily contaminating groundwater (Hale et al., 2016; Mahinroosta and Senevirathna, 2020; Ross et al., 2018). Furthermore, many of the current treatment methods that might work on PFAS have significant trade-offs, such as being energy intensive as well as disturbing biodiversity and soil structure (Mahinroosta and Senevirathna, 2020; Ross et al., 2018; Sparrevik et al., 2011; Travar et al., 2020). Hence, there is a great need for more sustainable new technologies for soils contaminated by PFAS.

Stabilization of PFAS in soil by amendment with carbonaceous materials, such as biochar and activated carbon (AC), has shown great potential compared to other adsorbents (Bolan et al., 2021; Du et al., 2014; Söregård et al., 2019a, 2019b, Söregård et al., 2020). Some studies have shown that AC is a better sorbent than biochar for PFAS, although biochar also performs well on sorption of especially long-chain PFAS (Fabregat-Palau et al., 2022; Kupryianchuk et al., 2016b; Söregård et al., 2020; Zhang and Liang, 2022). However, Sparrevik et al. (2011) found that fossil-based AC had a higher environmental impact than biomass-derived AC in sediment remediation of polychlorinated dibenzodioxins and furans, using a Life Cycle Assessment (LCA) to evaluate the impact. The use of contaminated, bio-based wood

waste and sewage sludge-based biochars as sorbents in water treatment and stabilization of PFAS contaminated soil could be a promising alternative that is both sustainable and just as effective for PFAS sorption as AC (Aumeier et al., 2023; Krahn et al., 2023; Silvani et al., 2019; Sørmo et al., 2021). Krahn et al. (2023) documented the importance of sewage sludge biochars being more mesoporous in the 1.5–30 nm range and hence better PFAS adsorbents than wood biochars. Larger pore structures can also minimise sorption attenuation caused by the presence of soil and/or other contaminants (Krahn et al., 2023), which are factors that otherwise can reduce sorption strength through pore blocking and restriction of diffusion pathways (Du et al., 2014). However, previous studies on the adsorption of PFAS to AC and biochar, either sludge-based or wood-based, have only been conducted as batch sorption tests in water. The only exception so far is Navarro et al. (2023) who found that wood-based biochars performed less well at reducing PFAS leaching from soil than commercial AC. Therefore, the ex situ and in situ performance of activated wood- and especially sludge-based biochar in a PFAS contaminated soil via column leaching studies currently constitutes a knowledge gap.

The main aim of the present work was thus to study effects of different sewage sludge- and wood-based biochars on the sorption and transport of PFAS from AFFF-affected soil, through up-flow column percolation tests. This was achieved by considering the following research objectives: 1) confirm if sewage sludge-based biochar will reduce PFAS leaching more effectively than (nonactivated) wood-based biochar due their higher SA and PV in the 1.5–30 nm pore size range, as a follow up to Krahn et al. (2023), 2) test whether activated biochar will sorb both PFAS and DOC to a larger extent than the nonactivated biochars, due to its higher specific surface area in the right pore size range; and 3) test if weakening or attenuation of PFAS sorption to sludge-based biochars in the presence of soil and a mixture of other PFAS and precursors commonly found in AFFF contaminated soil in a column system occurs to a similar extent as recently shown in a batch system (Krahn et al., 2023). This is the first study looking at sludge-based biochars and waste-based activated biochars as sorbents in field-contaminated PFAS-contaminated soil, and the first soil-PFAS-biochar study based on field-relevant column tests.

## 2. Materials and methods

### 2.1. Chemicals

Chemicals used for sample extraction and analysis included three isotopically labelled internal standards (IS) purchased from Cambridge Isotope Laboratories: PFOS-<sup>13</sup>C<sub>8</sub> (99 %), PFOA-<sup>13</sup>C<sub>8</sub> (99 %) and 6:2 FTS-<sup>13</sup>C<sub>2</sub> (99 %). HPLC gradient grade methanol (>99.8 %) and ethyl acetate (EtOAc, >99.7 % v/v) from VWR Chemicals (Trondheim, Norway), and ammonium acetate (>98.0 %) from Merck (Darmstadt, Germany). Water was purified using a Milli-Q grade Q-option Elga Labwater system (Veolia Water Systems LTD, U.K.).

PFAS analysis included 39 target analytes (TAs). A complete list of acronyms, CAS numbers, molecular structure and weights of the 39 TAs and the three internal standards (IS) is included in the supporting information (Table S.4). The TAs are categorized as either short-chain

( $\leq 6 \times$  perfluorocarbons – CF) or long-chain ( $> 6 \times$ CF) as according to Buck et al. (2011).

## 2.2. Contaminated soil

The PFAS-contaminated soil used in this study originated from a former firefighting training facility located at a Norwegian civil airport in the Oslo region where AFFF had been used. The area has glaciofluvial deposits mainly dominated by sand. For more details about the site see Høisæter et al. (2019) and Høisæter and Breedveld (2022). Soil from AFFF impacted hot-spots had previously been excavated and deposited at a waste handling site, where it was stored dry until it was subsampled for the present study by randomized multiple grab sampling. The soil was dried for approximately 48 h at 60 °C and manually sieved to remove large fibres and grains ( $> 4$  mm). The soil studied was a medium sand with a low TOC content ( $0.57 \pm 0.04$  %), a pH of  $6.2 \pm 0.1$ , and Al and Fe concentrations of  $29.7 \pm 0.6$  and  $21.3 \pm 0.6$  g/kg respectively.

## 2.3. Feedstocks for biochar sorbents

Six biochars were made in an industry-relevant medium-sized pyrolysis unit, including one from a clean biomass feedstock (clean wood chips, CWC) and five from contaminated organic waste feedstocks (Table 1). The contaminated organic waste feedstocks included sewage sludges from three different wastewater treatment plants (WWTP), one of which were contaminated with PFAS from the same source as the contaminated soil just described, and one type of contaminated wood waste/residues. The four contaminated feedstocks used to produce the biochars were analysed by Sørmo et al. (2023) and found to all contain PFAS prior to pyrolysis ( $55.6$ – $3651$   $\mu\text{g}/\text{kg}$ ). The resulting biochars, on the other hand, only had trace concentrations of PFAS ( $\leq 1$   $\mu\text{g}/\text{kg}$ ). The various feedstocks were dried and pelletised to  $40 \times 8$  mm prior to pyrolysis. Detailed descriptions and characteristics of the four nonactivated waste-based biochars and the reference biochar can be found in Sørmo et al. (2023), while the aWT is described in Sørmo et al. (2021).

## 2.4. Pyrolysis and activation

Production of the nonactivated biochars was done with an electrically heated Biogreen© medium scale (1–5 kg biochar per hr) pyrolysis unit made by ETIA Ecotechnologies, now part of VOW ASA (Lysaker, Norway). The activated aWT biochar was produced with an experimental pyrolysis unit PYREKA (Pyreg, Dörth, Germany) using a one-step pyrolysis and activation process to produce the aWT biochar, which was activated by adding a stoichiometric one-to-one ratio of  $\text{CO}_2$  to feedstock carbon. The pyrolysis technology and operational conditions are described in detail by Sørmo et al. (2023) for the ETIA-unit and Sørmo et al. (2021) for the PYREKA-unit. The 6 biochar samples were milled to a fine powder ( $D < 1$  mm) in a Retsch ISO 9001 ball mill at 80 rpm for 10 min. Despite applying the same milling process to all samples, the particle size distribution of the biochar sorbents could vary, and

subsequently impact sorption kinetics.

## 2.5. Column leaching tests

Leaching tests were carried out as up-flow column percolation tests, in accordance with EN 14405 (2017), as described in Høisæter and Breedveld (2022), but with a few modifications: Eight columns (poly-methylmethacrylate, height 50 cm, internal diameter = 5 cm) were packed with AFFF-impacted soil ( $\approx 850$  g) mixed with 1 % (w/w) biochar, while one column served as control with no biochar amendment. Mixing was done by adding soil and biochar to PE bags that were sealed and vigorously shaken. A triplicate column with DWSS biochar amended soil was included to estimate method uncertainty. Identical top and bottom lids made of polyoxymethylene (POM), with a polypropylene (PP) grid (to ensure uniform flow) and a  $0.45$   $\mu\text{m}$  polyether sulfone (PES) membrane filter closed the columns at each end. Separate leachate samples in separate bottles were collected from all columns at 6 different liquid-to-solid ratios (L/S; 0.1, 0.2, 0.5, 1, 2 and 5) achieved by pumping water (total volume  $\approx 4.25$  L) through the columns containing 850 g of soil, replacing about 16 pore volumes in total. Initially, the columns were saturated with Milli-Q water which was pumped from the bottom to the top of the columns and left for 5 to 6 days to equilibrate. After equilibration, Milli-Q water was pumped through at an average flow rate of 12.3–12.7 mL/h for about 15 days, while leachate was collected in separate HDPE bottles at the discrete time points when the respective L/S ratios had been achieved. The L/S ratio hence describes the amount of water (per mass) that has passed through the column relative to the mass of solids (d.w.) in the column. Sampling times were determined by monitoring the weight of the leachate. The leachate samples were split into the separate subsamples needed for the subsequent chemical analyses and measurements. Due to the low volume the L/S 0.1 samples were diluted (x-y times) before subsampling. After the end of the experiment, the leached soil ( $\approx 100$  g) was sampled from each column and analysed for mass balance purposes.

## 2.6. Sample preparation and instrumental analysis

### 2.6.1. PFAS extraction and analysis

Two extraction methods (one for solids and one for leachates) and one instrumental method were applied for the analysis of the 39 PFAS TAs. See the supporting information for a detailed list (Table S.4).

Target analytes were extracted from the leachate samples by solid-phase extraction (SPE), as described in Arvaniti et al. (2014). In short, 50 mL of the aqueous samples (mobile phase) were concentrated into solvent extracts, by passing them through Strata™-X Polymeric cartridges (200 mg/ 6 mL) from Phenomenex with a surface modified styrene divinylbenzene as sorbent polymer (stationary phase) followed by extraction using MeOH, up-concentration, and reconstitution to  $\sim 0.5$  mL. Soil-biochar samples were prepared for analysis by liquid-solid extraction (LSE), as described in Sørmo et al. (2023) based on Asimakopoulos et al. (2014). Briefly, target analytes were extracted

**Table 1**

Description of the different waste materials used as feedstocks for biochar, the temperature and residence time of pyrolysis.

Feedstock	Abbrev.	Description	Pyrolysis temperature (°C)	Pyrolysis residence time (min)
Clean wood chips	CWC	Wood pellets produced from logging and forestry residues, mainly pine and spruce.	700	20
Digested sewage sludge 1	DSS-1	A waste product after anaerobic digestion of sewage sludge and food waste for biogas production.	700	20
Digested sewage sludge 2	DSS-2	A waste product after anaerobic digestion of sewage sludge for biogas production.	800	20
De-watered sewage sludge	DWSS	De-watered raw sewage sludge, thermally hydrolysed at 170 °C followed by centrifugation at 100 °C.	700	40
Waste timber	WT	Various wood products discarded by citizens and businesses (no impregnated wood).	800	20
Activated waste timber	aWT	Same feedstock as WT but activated with $\text{CO}_2$ on a 1:1 stoichiometric ratio with feedstock carbon.	900	12

from 0.2 g of the solid matrix in ethyl acetate and ammonium acetate buffer by ultrasound-assisted extraction (UAE) followed by centrifugation and up-concentration. All sample extracts were analysed using ultra-high performance liquid chromatography coupled with a Xevo TQ-S triple quadrupole mass spectrometer (UPLC-MS/MS) equipped with a Z spray ESI in negative mode. Instrumental parameters are specified in supporting information.

### 2.6.2. Additional characterization

Analysis of dissolved organic carbon (DOC) in leachate samples and total organic carbon (TOC) in soil samples were carried out following EN 1484 (1997) and EN 13137 (2001) for DOC and TOC, respectively.

Surface area (SA) and pore volume (PV) were determined by CO<sub>2</sub> gas adsorption and DFT data evaluation for pores 0.3–1.5 nm, while N<sub>2</sub> gas adsorption and BET- (for SA) and BJH (for PV) data evaluation were used for pores >1.5 nm. Both CO<sub>2</sub> and N<sub>2</sub> gas adsorption spectrometry were carried out using a Quantachrome Autosorb iQ analyzer.

Total carbon in the biochars was analysed using dry combustion at 1030 °C followed by element analysis with IR detection on a Leco CHN628 instrument, described by Nelson and Sommers (1983).

Elemental analysis of biochar sorbents were determined in triplicates by nitric acid (HNO<sub>3</sub>, conc.) microwave digestion (260 °C, Ultraclave, Milestone), and triple quadrupole (QQQ) induced coupled plasma mass spectrometry (QQQ ICP-MS, 8800, Agilent Technologies) for As, Ba, Cd, Co, Cr, Cu, Mo, Ni, Pb, S, Sr and V, and ICP optical emission spectrometry (ICP-OES, 5100, Agilent Technologies) for Ca, Fe, K, Mg, Na, P, Si and Zn. Column leachate samples were acidified (10 % HNO<sub>3</sub>) before direct analysis by ICP-MS or ICP-OES.

Briefly, condensed aromatic carbon (ConAC) contents were quantified through benzene polycarboxylic acids (BPCA) analysis. Samples were digested (65 % nitric acid (HNO<sub>3</sub>); 170 °C; 9 h), after which HNO<sub>3</sub> was evaporated, and the residue dissolved in phosphoric acid (H<sub>3</sub>PO<sub>4</sub>; 0.6 M). Benzenepentacarboxylic acid (B5CA) and benzenhexacarboxylic acids (B6CA) were quantified by HPLC (Agilent 1100; detection at 254 nm) according to Wagner et al. (2017). B6CA + B5CA gave ConAC using a conversion factor of 7.04 (Bostick et al., 2018). The B6CA and B5CA amounts were used to estimate the ConAC fractions in the biochars using a conversion factor of 7.04:

$$\frac{\text{ConAC}}{\text{solid}} (\%) = \frac{(\text{B6CA}_{\text{produced}}(\text{mg}) + \text{B5CA}_{\text{produced}}(\text{mg})) \times 7.04}{m_{\text{sample}}(\text{mg})} \times 100 \quad (1)$$

### 2.7. QA/QC

Three internal standards (IS; PFOS-<sup>13</sup>C<sub>8</sub>, PFOA-<sup>13</sup>C<sub>8</sub> and 6:2 FTS-<sup>13</sup>C<sub>2</sub>) were added to all samples pre extraction to assess recovery and matrix effects. Procedural blanks (both for leachate and soil) and certified reference material (CRM, Domestic Sludge 2781, National Institute of Standards and Technology, USA) were spiked either pre- or post-extraction to evaluate background contamination, in addition to obtain absolute recoveries (AR%), relative recoveries (RR%) and matrix effect (ME%).

During UPLC-MS/MS, solvent blanks (MeOH) were injected at regular intervals and analysed to monitor for cross-contamination and carryover. A calibration standard solution at 5 ppb was also analysed to monitor potential signal drifting. A solvent mixture (MeOH:Milli-Q, 50:50 v/v; FA, 0.1 %) was used for pre- and post-injection wash of the injection needle.

Standard calibration solutions spanned from 0.01 to 100 µg/L. The internal standard method and matrix-matched calibration standards (see Hubert et al. (2023)) were used to quantify PFAS concentrations and to assure greater accuracy in the measurements in addition to compensating for losses during sample preparation and analytical errors as matrix effects and losses during the extraction.

Sorption losses to tubes and vials were tested to be negligible to low during the previous studies (Krahn et al., 2023; Sørmo et al., 2021) and

certainly would not influence the present data due to the high initial PFAS concentrations in the soil.

A description and recovery percentages of AR, RR and ME (Table S.5), in addition to other QA/QC protocols is presented in Section S.1 in the supporting information for; the reference material certificate is presented in Section S.2.

Method error (column test) and sampling error (leachate sampling) was estimated, respectively, by setting up one of the columns in triplicate (DWSS) and by splitting samples from another one of the columns (CWC) into triplicates. The standard deviations calculated from these two sets of triplicate samples were applied as a partial measure of uncertainty, through extrapolation, to the single columns run without replicates.

### 2.8. Data analysis

The content of PFAS leached from the soil (C<sub>leachable</sub>) was defined as the amount of PFAS released during the experiment per dry weight of soil in the column, given as:

$$C_{\text{leachable}} [\mu\text{g kg}^{-1}] = \frac{C_w [\mu\text{g L}^{-1}] \times V_w [\text{L}]}{M_{\text{soil,dw}} [\text{kg}]} \quad (2)$$

Where C<sub>w</sub> is the concentration of PFAS in the eluate, V<sub>w</sub> is the volume of the eluate and M<sub>soil,dw</sub> is the mass of the soil in the column in dry weight.

The reduced leaching of PFAS in soil with biochar amendment relative to unamended soil is given as:

$$\text{Reduction} [\%] = \left( \frac{C_{\text{leachable,unamended}} [\mu\text{g kg}^{-1}] - C_{\text{leachable,biochar}} [\mu\text{g kg}^{-1}]}{C_{\text{leachable,unamended}} [\mu\text{g kg}^{-1}]} \right) \times 100 \quad (3)$$

A 1st order non-linear model was used based on a contaminant leaching model:

$$M(t)_{\text{modelled}} [\mu\text{g}] = M(0)_{\text{measured}} [\mu\text{g}] \times e^{-k_{\text{PFAS}} [\text{min}^{-1}] \times t [\text{min}]} \quad (4)$$

It is noted that a 1st order non-linear model is appropriate for the test conditions here being homogeneously distributed analytes over the entire volume of the column, which is uniformly flushed out following 1D flow, based on the retardation due to desorption. For other types of column studies where the contaminant is introduced to at the beginning of the column flow, and not homogeneously through the entire column as here, the convection-dispersion equation would be more appropriate. Eq. (4) was solved by adjusting the desorption rate constant, k<sub>PFAS</sub> (see Table S.15), by minimizing the cumulative squared error between ln(M(t)<sub>measured</sub>) and ln(M(t)<sub>modelled</sub>). The retardation factor (R) (see Table S.17) and distribution coefficient, K<sub>d,tot</sub> were determined by isolation from the following equations, using the bulk density (ρ<sub>b</sub>) and porosity (θ) of the soil, as well as the water percolation rate in column volumes per minute (min<sup>-1</sup>), k<sub>w</sub>:

$$k_{\text{PFAS}} [\text{min}^{-1}] = \frac{k_w [\text{min}^{-1}]}{R [-]} \quad (5)$$

$$R [-] = 1 + \left( \frac{K_{d,\text{tot}} [\text{L kg}^{-1}] \times \rho_b [\text{g mL}^{-1}]}{\theta [-]} \right) \quad (6)$$

Sorption coefficients for the biochar only (K<sub>d,BC</sub>) were derived using a mass balance describing the percentage of biochar and soil in the column:

$$K_{d,\text{tot}} = K_{d,\text{soil}} \times 0.99 + K_{d,\text{BC}} \times 0.01 \quad (7)$$

See Section S.1 in supporting information for a more detailed description of the model.

Attenuation factors (AF) for individual PFAS to the biochar sorbents were estimated using log K<sub>d,BC-soil-mix</sub> values (from the present work with soil and other PFAS) calculated using the approach described above



(Eqs. 4–6) and log  $K_{d,BC-single}$  values (for clean biochar without soil and without other PFAS) calculated using log  $K_{F,BC}$  (Freundlich isotherm for single PFAS in water) from Krahn et al. (2023).  $K_{F,BC}$  values from single PFAS-water batch tests at  $C_w$  of 1  $\mu\text{g/L}$  from Krahn et al. (2023) were used to calculate  $K_{d,BC-single}$  values. It should be noted that these AFs are imperfect estimates, as the  $K_d$ -values applied in the calculation stem from different systems (batch test and column test). Although the timeframes (14 days for batch test and 15 days for the column test) were similar, the L/S ratios differed (10 for batch tests and 5 for column tests) and there might be differences in sorption kinetics, as the batch test involves intensive shaking at a given L/S ratio, while the column tests are operated with a continuous supply of water up through an undisturbed, packed soil column until a given L/S ratio is reached. AF were calculated for PFHxA, PFHpA and PFOA to the CWC, DSS-1 and DWSS biochars, as this selection of congeners and sorbents were included in both the present and the Krahn et al. (2023) studies (unfortunately PFOS was not included in Krahn et al. (2023)):

$$AF = \frac{K_{d,BC-single} \text{ (Krahn et al., 2023)}}{K_{d,BC-soil-mix} \text{ (this work)}} \quad (8)$$

Attenuation factors thus represent how much weaker sorption to the biochars is in the presence of soil and other PFAS under column test conditions, which is more representative of leaching in soil, as compared to sorption of single PFAS to clean biochars in a batch test, which gives an upper level to sorption, as shaking allows for more kinetic access to deeper pores in the biochar.

The relative volumes of water applied in the column leaching test, were converted into years of precipitation through the simplified estimation shown in Eq. 9 (Van der Sloot et al., 1984). Eq. 9, estimates the number of years ( $t$ , y) for the soil to be exposed to the same amount of water as applied in the column test, based on the L/S ratio (L/kg), and the mean annual precipitation ( $N$ , mm/y), soil bulk density ( $d$ , kg/m<sup>3</sup>), and depth to groundwater ( $h$ , m):

$$t(y) = \frac{L/S \text{ (L/kg)} \times d \text{ (kg/L)} \times h(m)}{N(m/y)} \quad (9)$$

### 3. Results and discussion

#### 3.1. Unamended soil, biochar and leachate properties

A total of 29 of the 39 PFAS target analytes were detected across all leachate and soil samples (Table S.13 and S.14). In the unamended soil (before leaching), 24 different PFAS ( $\sum\text{PFAS}_{24}$ ) were detected with a total concentration of  $1329 \pm 46 \mu\text{g/kg}$  ( $n = 3$ ), of which 88 % were PFOS (Fig. S.2). Data will be presented and discussed for PFOS and a selection of 9 other PFAS (PFBS, PFHxS, PFHxA, PFHpA, PFOA, 6:2 FTS, 8:2 FTS, PFOSA, and diSAMPAP), which were detected in leachate from the control column at relatively high concentrations (i.e.,  $>1 \mu\text{g/L}$ ) while representing a variation in chain length (4xCF to 16xCF) and congener type (PFSA, PFCA, FTS, fluorosulfonamide (FSA) and per-fluorosulfonate phosphate esters (SAMPAP)) (Table S.4).

The carbon contents of the three wood-based biochars were all above 85 %, almost three times higher than those of the sludge-based biochars (Table S.6). The sludge-based biochars, on the other hand, had higher ash contents (73.4–93.4 %), compared to the three wood-based biochars (3.73–15.5 %). Sludge feedstocks contain more inorganic material and more volatile organic carbon species than wood feedstocks, resulting in sludge biochars having higher ash and lower carbon contents, and generally higher yields (Ahmad et al., 2014; Zhang et al., 2013).

Fig. 1 presents the cumulative leaching of PFOS per kg of soil from the unamended and amended columns from L/S 0.1 to 5. The relative time it would take for the soil to be exposed to the same amount of water given field conditions (per Eq. 9) is also shown. Over the course of 33 years 3000  $\mu\text{g/kg}$  of PFOS could leach from the unamended soil to groundwater, compared to 32–253  $\mu\text{g/kg}$  from the soils amended with DSS-1, DSS-2, DWSS and aWT biochars. Examples of leaching curves for other congeners can be found in the SI (Fig. S.1).

The total leachable  $\sum\text{PFAS}_{24}$  concentration was 3088  $\mu\text{g/kg}$ , which was more than double the concentration extracted from the original soil ( $1329 \pm 46 \mu\text{g/kg}$ ). This large variation may be due to i) heterogeneity of the original soil, ii) transformation of precursor compounds, and/or iii) insufficient extraction. However, the low 2–3 % standard deviation in the soil extraction ( $1329 \pm 46 \mu\text{g/kg}$ ) falsifies the heterogeneity hypothesis, and the recoveries observed (Table S.5) suggest sufficient extraction. Thus, the most likely explanation is transformation of precursor compounds during the course of the experiment. The uncertainty

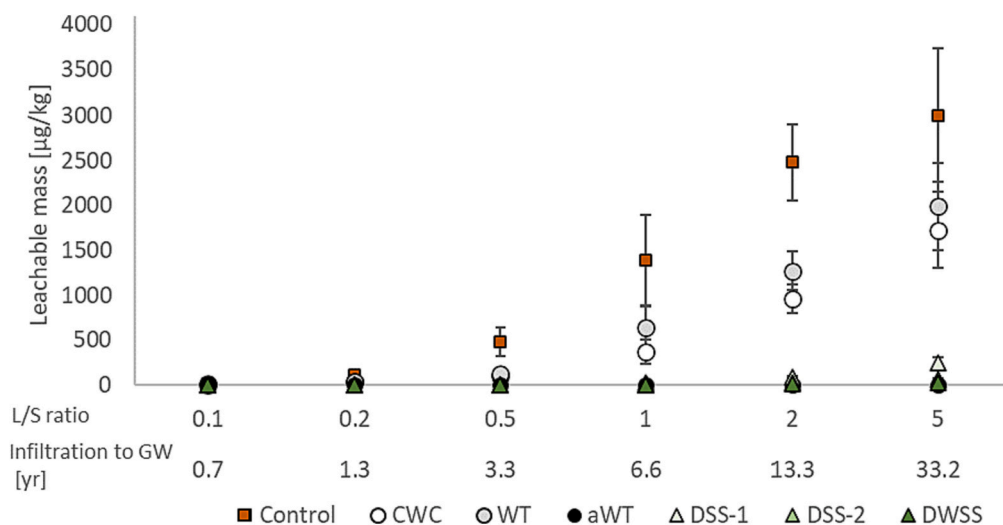


Fig. 1. Cumulative leachable mass of PFOS per kg of soil in the over the L/S ratios 0.1 to 5 in column leaching test with unamended soil and soil (Control) and soil amended with clean wood chips (CWC), waste timber (WT), activated waste timber (aWT), digested sewage sludges (DSS-1 and DSS-2), and de-watered sewage sludge (DWSS) biochars (1 %). Also displayed is the equivalent amount of time it would take for this L/S ratio to be reached in a soil column with precipitation  $N = 750 \text{ mm/yr}$ , bulk density  $\rho_b = 1.44 \text{ kg/m}^3$ , and depth to groundwater = 1.0 m (eq. 9). Error bars represent relative standard deviations based on partial measures of uncertainty.

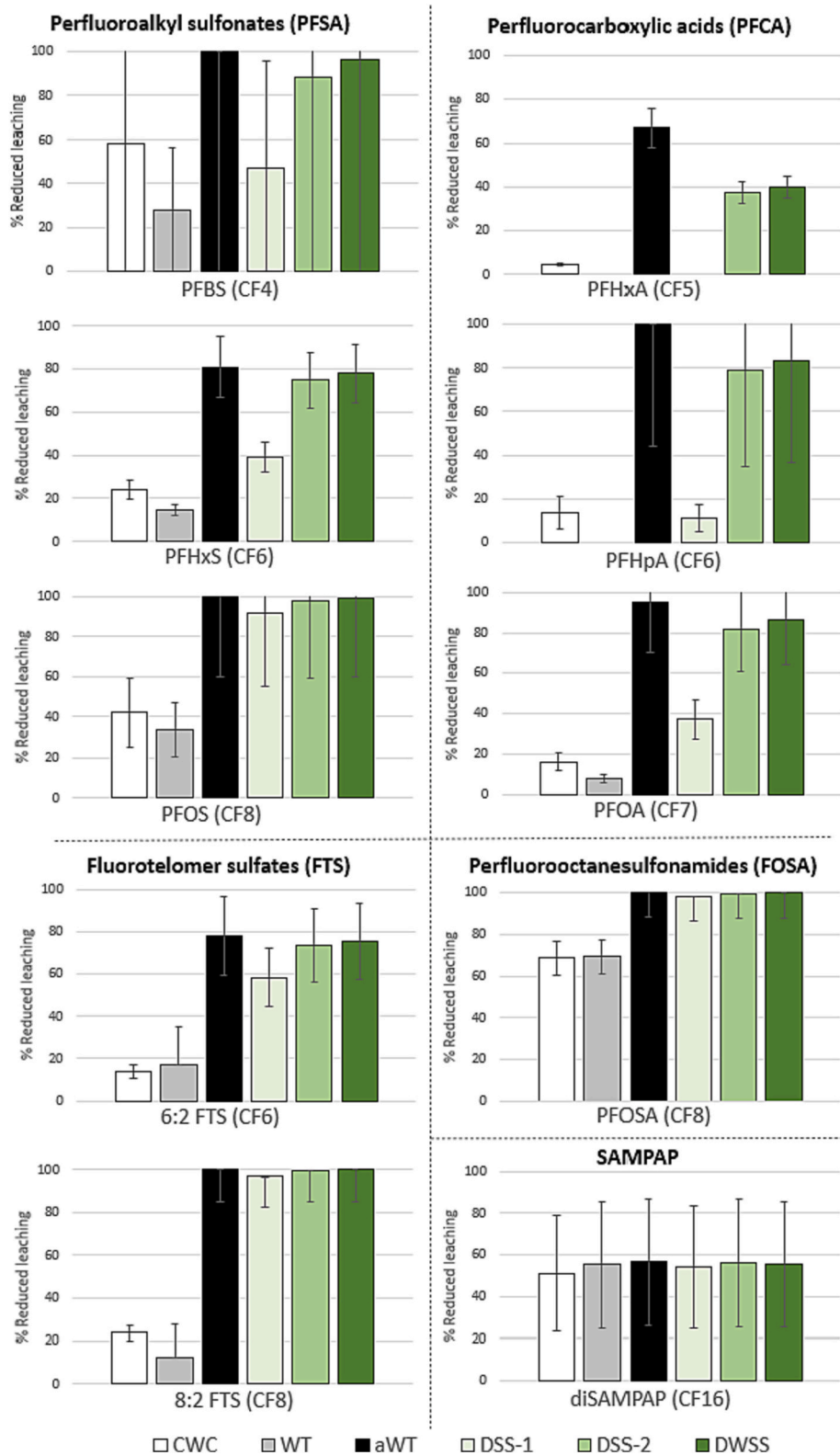


Fig. 2. Reduction [%] in leaching of PFAS by amendment with clean wood chips (CWC), waste timber (WT), activated waste timber (aWT), digested sewage sludges (DSS-1 and DSS-2), and de-watered sewage sludge (DWSS) biochar sorbents, relative to the control. The graphs are grouped by the PFAS functional group. CFx refers to the number of perfluoroalkyl carbons. Error bars represent relative standard deviations based on partial measures of uncertainty.

in total PFAS concentration gives a systematic uncertainty of 0.4 log units to the  $K_d$ -values to be reported in the forthcoming sections. Relative differences between treatments remain the same, but absolute numbers could be slightly different from the ones reported.

### 3.2. Reduction of PFAS leaching by biochar amendments

Strong reductions in PFOS leaching from the soil, relative to the control column, were observed upon amendment with most biochars; 99.9 % for aWT,  $98.9 \pm 0.2$  % for DWSS, 97.8 % for DSS-2 and 91.6 % for DSS-1 biochars, respectively. In contrast, lesser reductions in PFOS leaching were observed for the CWC ( $42.4 \pm 5.1$  %) and WT (33.7 %) biochars (Fig. 2). For other PFAS, the same overall trend was observed, with aWT and sludge-based biochars demonstrating the strongest reductions in PFAS leaching. Importantly, the strong effectiveness of the sludge-based chars for PFAS retention reflects the observations of Krahn et al. (2023) who observed strong removal of PFAS from aqueous systems by these sorbents, with  $K_d$ -values almost as high as those for commercial activated carbons. While two of the sludge biochars, DWSS and DSS-2, demonstrated relatively strong abilities for reducing PFAS leaching, the DSS-1 sample, on the other hand, had a significantly poorer performance (Fig. 2). It is argued that this difference is due to a lower PV and SA available for sorption of large PFAS molecules (see Section 3.3). The high effectiveness of the activated aWT biochar in the present column tests corresponds to previous results by Sørmo et al. (2021) for the same sorbent, reporting substantial reduction in PFAS leaching in batch tests (>99 %) in batch tests with low-TOC soil (0.34 % TOC) at varying biochar doses (1–5 %).

Potential limitations to the remediation effectiveness of the biochar sorbents were, however, observed, as long-chain PFAS (>6 x CF<sub>2</sub>) were retained more effectively than short-chain anionic PFAS ( $\leq 6$  x CF<sub>2</sub>), e.g. PFOA (95 %) vs. PFHxA (67 %) for aWT (Fig. 2). This observation is novel for soil-amended sludge biochars and similar to earlier observations of other, single biochars or sludge biochars in aqueous systems, where it has been explained by weakened hydrophobic interactions due to the lower hydrophobicity of the shorter fluorocarbon chains and similar electrostatic repulsion between the negatively charged PFAS head groups and biochar surfaces (Fabregat-Palau et al., 2022; Krahn et al., 2023; Söregård et al., 2019a, 2019b). Improvement of biochar retention of short-chain anionic PFAS is still being explored. For instance, a

recent study has suggested that modifications that increase electrostatic interactions between these short-chain PFASs and biochar surfaces, such as iron doping to provide a lower zeta potential, and possibilities for interactions between positively charged Fe-sites and anionic head groups of PFAS, could significantly improve biochar performance (Liu et al., 2023).

Logarithmic soil-water distribution coefficients varied between 0.10 and 1.26 for the unamended soil ( $\log K_{d,soil}$ ). Sorption to the biochars varied by over five orders of magnitude for the 10 different PFAS (Table 2), with  $\log K_d$  ranging from  $-0.07$  to  $\geq 3.48$  for biochar-amended soil ( $\log K_{d,tot}$ ), and from 0.26 to  $\geq 5.48$  for biochar only ( $\log K_{d,BC}$ ; total sorption to soil-biochar systems corrected for sorption to the soil matrix).  $K_{d,BC}$  generally followed the same order for all congeners: WT < CWC < DSS-1 < DSS-2 < DWSS < aWT. Because of the weak sorption of short-chain PFAS, only a few  $K_{d,BC}$  values could be calculated for this compound, with the following order of increasing sorption: DSS-1 < DWSS < DSS-2. The tendency of lower removal efficiencies of short-chain PFAS by both AC and wood-based biochars was also found by e. g., Eschauzier et al. (2012) (water treatment), Ross et al. (2018) and Zhang and Liang (2022) (soil treatment).

### 3.3. PFAS sorption capacity and biochar pore sizes

Overall sorption strength is the combination of sorption capacity and affinity. Biochar pore volume (PV) has been shown to be one the most important characteristic affecting the sorption capacity of various organic contaminants (Fabregat-Palau et al., 2022; Hale et al., 2016; Krahn et al., 2023). The pore size distribution can have a great impact on the sorption capacity of organic contaminants, as it is important if the sorbates can enter and sorb to the surface area within the pores and avoid size exclusion due to restricted diffusion. Zimmerman et al. (2004) studied micropore sorption of various organic molecules and found that a molecule will fit inside a pore that is larger than two times the diameter of the molecule. Given the molecular size of PFAS molecules of about 1–2 nm (Table S.9), biochar pores sizes of minimum 2–3 nm are required to accommodate the currently studied PFAS. The aWT and sludge biochars showed relatively large porosity in the >1.5 nm range (e.g. SA and PV for aWT of 617 m<sup>2</sup>/g and 0.429 cm<sup>3</sup>/g, and for DWSS of 128 m<sup>2</sup>/g and 0.126 cm<sup>3</sup>/g, respectively, Fig. 3).

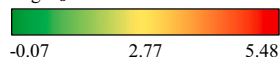
In contrast, the majority of the porosity in the CWC and WT biochars

**Table 2**

Log  $K_d$  values [L/kg] for the 6 different biochars and the control computed for 10 selected PFAS. Log  $K_d$  were calculated for both the soil ( $\log K_{d,soil}$ ), soil- 1 % biochar mixture ( $\log K_{d,tot}$ ), and for the biochar alone ( $\log K_{d,BC}$ ). Log  $K_d$  values for DWSS are given as mean values  $\pm$  standard deviation ( $n = 3$ ). \* = values computed using a 1st order two-compartment model (Section S.1, Supplementary Information, eq. 7 in SI). \*\* = mean value ( $n = 2$ ). NA =  $K_d$  could not be computed due to no detected PFAS concentration in leachate and/or soil, or due to no significant/measurable sorption of  $F_{rap}$  in the model. Values given as “ $\geq$ ” were calculated (partly) with leaching concentration of LOD/2, as very little or no leaching was observed. Note that the uncertainty in  $M(0)$  renders an additional systematic uncertainty of maximally 0.4 log units to the reported values.

Biochar type	Control	CWC		WT		aWT		DSS-1		DSS-2		DWSS		
Compound	CF-chain length	Log $K_{d,soil}$	Log $K_{d,tot}$	Log $K_{d,BC}$	Log $K_{d,tot}$	Log $K_{d,BC}$	Log $K_{d,tot}$	Log $K_{d,BC}$	Log $K_{d,tot}$	Log $K_{d,BC}$	Log $K_{d,tot}$	Log $K_{d,BC}$	Log $K_{d,tot}$ (n=3)	Log $K_{d,BC}$ (n=3)
PFBS	CF4	NA	NA	NA	NA	NA	NA	NA	$\geq -0.1$	NA	$\geq 1.5$	NA	$\geq 1.1^{**} \pm 0.2$	NA
PFHxA	CF5	$\geq 0.7^*$	NA	NA	NA	NA	$\geq 1.3$	$\geq 3.2$	$\geq 0.7$	NA	1.1	2.8	$1.2 \pm 0.1$	$2.9 \pm 0.2$
PFHpA	CF6	0.3*	NA	NA	NA	NA	2.3	4.2	0.4	1.8	1.3	3.3	$1.8 \pm 0.4$	$3.8 \pm 0.4$
6:2 FTS	CF6	1.3*	NA	1.2*	NA	1.4*	1.7	3.5	1.3	2.6	1.6	3.3	$1.7 \pm 0.1$	$3.4 \pm 0.1$
PFHxS	CF6	0.7*	NA	1.0*	NA	1.0*	1.6	3.6	0.9	2.6	1.5	3.4	$1.6 \pm 0.1$	$3.5 \pm 0.2$
PFOA	CF7	0.5*	NA	0.3*	NA	1.3*	2.3	4.3	1	2.8	1.6	3.5	$1.9 \pm 0.1$	$3.9 \pm 0.1$
PFOS	CF8	0.1	0.4	2.1	0.3	2	3.1	5.1	1	3	1.6	3.6	$2.1 \pm 0.1$	$4.1 \pm 0.1$
8:2 FTS	CF8	0.6	0.9	2.7	0.9	2.6	$\geq 2.9$	$\geq 4.9$	2.2	4.2	$\geq 2.8$	$\geq 4.8$	$\geq 2.8 \pm 0.1$	$\geq 4.8 \pm 0.1$
PFOSA	CF8	0.7	1.2	3	1	2.7	$\geq 3.5$	$\geq 5.5$	2.2	4.2	2.4	4.4	$\geq 3.2 \pm 0.5$	$\geq 5.2 \pm 0.5$
diSAMPAP	CF16	1	1.2	2.9	1.2	2.7	1.2	2.9	1.5	3.3	1.3	2.9	$1.4 \pm 0.1$	$3.2 \pm 0.1$

Log  $K_d$



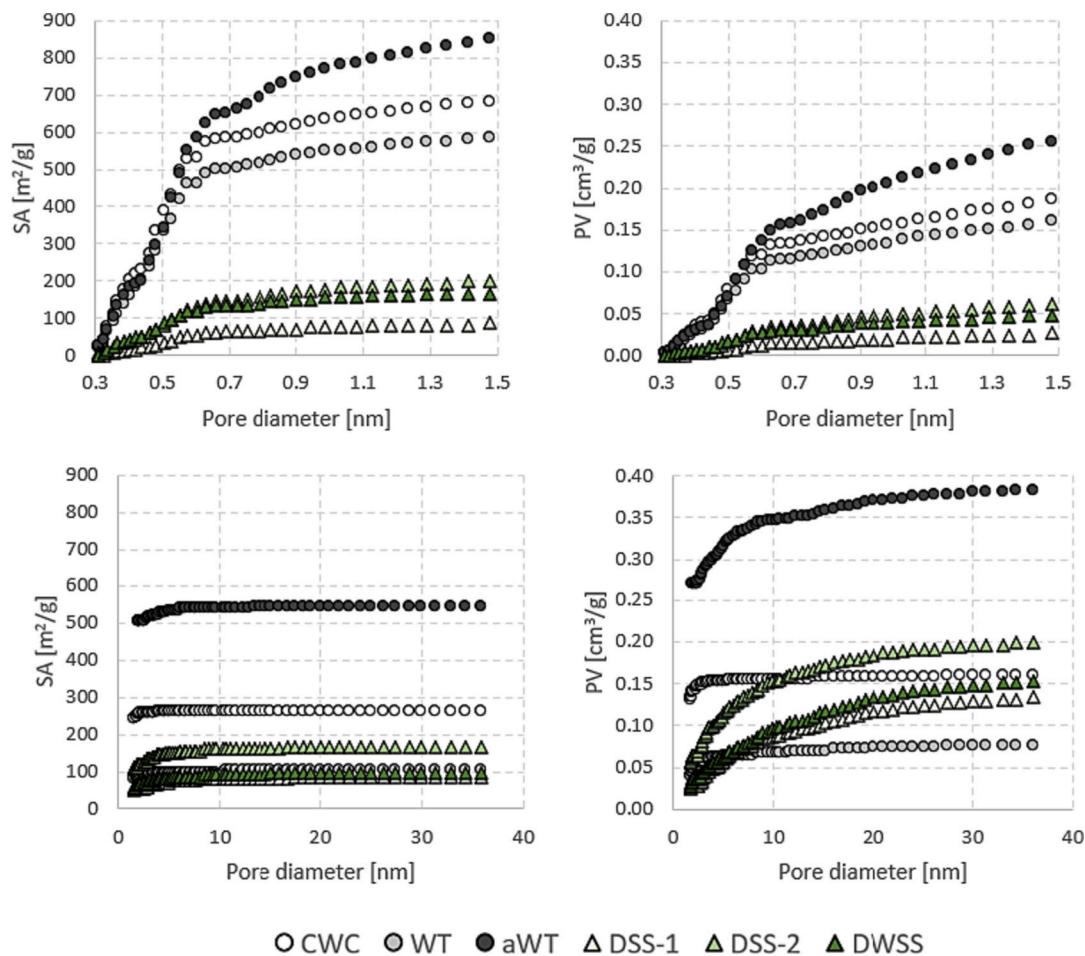


**Fig. 3.** Surface area (SA) given in  $\text{m}^2/\text{g}$  and pore volume (PV) in  $\text{cm}^3/\text{g}$  for pores between 0.3 and 1.5 nm and  $>1.5$  nm, for the clean wood chips (CWC), waste timber (WT), activated waste timber (aWT), digested sewage sludges (DSS-1 and DSS-2), and de-watered sewage sludge (DWSS) biochars.

(>72 % of PV and > 85 % of SA for pores between 0.3 and 1.5 nm (Table S.18)) were located in ultra-micropores (< 0.7 nm), or pores smaller than 3 nm (>90 % for CWC and > 75 % for WT of PV for pores  $>1.5$  nm (Table S.19)), resulting in too little porosity within a suitable size range to accommodate the large PFAS molecules, and thus severe size exclusion effects and relatively modest reductions in PFAS leaching. These differences likely also explain the variability in the performance of the sludge biochars, as the DSS-2, which were the better sorbent, had a SA in the  $>1.5$  nm pore size region about twice that of DSS-1 ( $\text{SA}_{>1.5 \text{ nm}} = 219 \text{ m}^2/\text{g}$  and  $\text{SA}_{>1.5 \text{ nm}} = 110 \text{ m}^2/\text{g}$  for DSS-2 and DSS-1 respectively, Fig. 3).

### 3.3.1. Link between sorption affinity and PFAS properties

Sorption affinity is determined by the interactions between PFAS and the biochar matrix. These interactions are the net result of net favourable hydrophobic dispersive interactions between the hydrophobic  $(\text{CF}_2)_n$  PFAS tails and the biochar (Du et al., 2014; Goss et al., 2006), which increases with chain length, and potential repulsion between negatively charged head groups (sulfonates, carboxylic acids) and mostly negatively charged biochar (Xiao et al., 2017).

In general, increase in  $K_d$  values with increasing CF-chain length was observed, which is in accordance with other studies (Fabregat-Palau et al., 2022; Higgins and Luthy, 2006; Hubert et al., 2023; Krahn et al., 2023; Sigmund et al., 2022; Söregård et al., 2020) and caused by the high free energy required for cavity formation per  $\text{CF}_2$  moiety in water, making it more energetically favourable to adsorb to the biochar surface.

For PFAS with similar perfluorinated chain lengths,  $K_d$  generally

increased in the following order: carboxylic acid < sulfonic acid < fluorotelomer < sulfonamide. This trend was observed for three PFAS with CF-chain length of 8 (PFOS, 8:2 FTS and PFOSA), with  $\log K_{d,BC}$  values for e.g. DWSS:  $4.10 \pm 0.11 < 4.83 \pm 0.13 < 5.22 \pm 0.52$ , respectively. A similar order of increasing  $K_d$  values (PFOS < 8:2 FTS < PFOSA) was reported by Hubert et al. (2023). These authors suggested that the stronger sorption of the telomeric functional head group could be explained by its weaker negative charge, compared to that of the sulfonic acid. This weaker negative charge results in weaker repulsion of the 8:2 FTS head group by the negatively charged biochar surface. It was furthermore suggested by Hubert et al. (2023) that the sulfonamide head group on PFOSA becomes partially neutral at environmental pHs, due to a relatively high  $\text{p}K_a$  of approximately 6.2 compared to <0.3 and - 2.6 (Nguyen et al., 2020) for PFOS (Rayne and Forest, 2016; Vierke et al., 2013) and 8:2 FTS (Nguyen et al., 2020), respectively. This leads to lower water solubility and decreased electrostatic repulsion and thus stronger sorption to negative charged biochar surfaces. The trends in  $K_{d,BC}$  values in the present study (Table 2) probably indicate that hydrophobic interactions are the dominant sorption mechanism for long-chain PFAS. These interactions are less strong for short-chain PFAS, allowing the head group repulsion to exert a relatively strong effect on the overall sorption effect of short-chain PFAS.

These results demonstrate the interplay between affinity and capacity in determining the overall effectiveness of the biochar sorbents. Long-chain PFAS will sorb strongly, due to high affinity, but only when there are sufficient available pores within a suitable size range (capacity). This could explain the relatively lower sorption of diSAMPAP, which is the largest of PFAS considered, having a weaker sorption than



PFOS, due to size exclusion into the pores. Short-chain PFAS, on the other hand, do not necessarily experience the same degree of size exclusion effects, but will nevertheless sorb poorly due to a lower affinity.

Generally, a higher condensed aromatic carbon content (ConAC) of biochars has been found to result in stronger sorption of PFAS and other organic compounds (Fabregat-Palau et al., 2022; Kupryianchuk et al., 2016a; Zhang et al., 2021). The aromaticity of biochars has mainly been found to increase with pyrolysis temperature (Wiedemeier et al., 2015), and 700 °C has been identified as an important threshold at which graphitic regions begin to fuse into clusters of condensed aromatic carbon (Pignatello et al., 2017). In the present study, all biochar sorbents were produced at temperatures  $\geq 700$  °C, and although the total carbon contents of the sludge-based biochars (13.5, 27.7, and 29.6 % for DSS-1, DSS-2, and DWSS respectively) were much lower than those of the wood based biochars (91.4, 85.1 and 89.5 for CWC, WT, and aWT respectively), there were no significant differences in ConAC contents (79–86 %, Table S.6) among all biochars tested. This demonstrates that the pyrolysis temperatures applied were sufficient to transform the majority of the carbon present in the biochars to highly condensed aromatic structures, and subsequently, that the biochar sorbents likely have similar affinities for the sorbates. Thus, the difference in sorption effect observed in the present work, is most likely owing to a difference in capacity and not affinity, due to the availability of surface area and pore volume within a suitable pore size range.

### 3.4. Relationship between DOC and PFAS leaching

DOC concentrations in leachate samples decreased with higher L/S ratios, linearly ( $R^2 = 0.95$ ) for the control column without biochar, from  $160 \pm 47$  mg/L at L/S 0.1 to  $16 \pm 0.7$  mg/L at L/S 5. DOC concentrations at L/S 0.1 for the same soil amended with the various biochars showed a strong variation in the following manner: WT ( $191 \pm 55$  mg/L)  $\geq$  CWC ( $176 \pm 51$  mg/L)  $\geq$  control ( $160 \pm 47$  mg/L)  $>$  DSS-1 ( $73 \pm 21$  mg/L)  $>$  DWSS ( $52 \pm 15$  mg/L)  $>$  DSS-2 ( $31 \pm 8.9$  mg/L)  $>$  aWT ( $19 \pm 5.6$  mg/L). The same trends were observed at the other L/S ratios (Fig. 4 and Table S.11), indicating DOC binding by the aWT and sludge

biochars but not by the wood biochars. Amendment with biochar has previously been documented to lower the DOC concentrations compared to unamended soil (Smebye et al., 2016; Sørmo et al., 2021; Thies and Rillig, 2009). The opposite trend was found by Tang et al. (2019), who reported increasing DOC concentrations with biochar amendment in soil, explained by DOC release from biochar rather than sorption to it.

Through the whole leaching cycle, maximally 130 mg DOC was leached per kg of soil (control and WT soils) from a total of 0.57 % C = 5700 mg of DOC (per kg of soil). Approximately 2.2 % of total C was leached during the whole experiment for the non-amended and wood char amended soils. For the soils amended with the most strongly sorbing biochars (aWT and DSS-2), 30 mg was leached from a total of 8000–14,000 mg of OC (0.2–0.4 % of total C). This shows that the net effect of biochar was retention of DOC – in other words, the DOC binding by the biochars outweighed the amount of DOC desorbing from the biochars during the experiment.

### 3.5. Attenuation factors

For all biochar/PFAS combinations, weaker sorption was observed in the soil-PFCA systems in the present study than in previously studied batch /water systems containing the same biochars and looking exclusively at PFCAs (Krahn et al., 2023), indicating significant weakening, or attenuation, of the PFCAs sorption to the biochar due to the presence of other compounds/PFAS congeners and/or soil (Cornelissen and Gustafsson, 2006; Krahn et al., 2023; Werner et al., 2006). However, it should be mentioned that these previous tests were done using a batch equilibrium system and shaking, which can have different biases compared to up-flow percolation tests, such as different L/S ratio, altered soil structures from batch test shaking and/or possible preferential flow paths or non-equilibrium kinetics in the up-flow percolation tests, which collectively and potentially lead to stronger sorption in batch experiments. Furthermore, pH differed in the column test leachate, compared to the batch study, due to the different biochar doses (1 % and 2 % respectively) and soil types applied. This could create a slight bias as a higher pH will likely result in weaker sorption of anionic PFAS due to increased repulsion from the negatively charged biochar

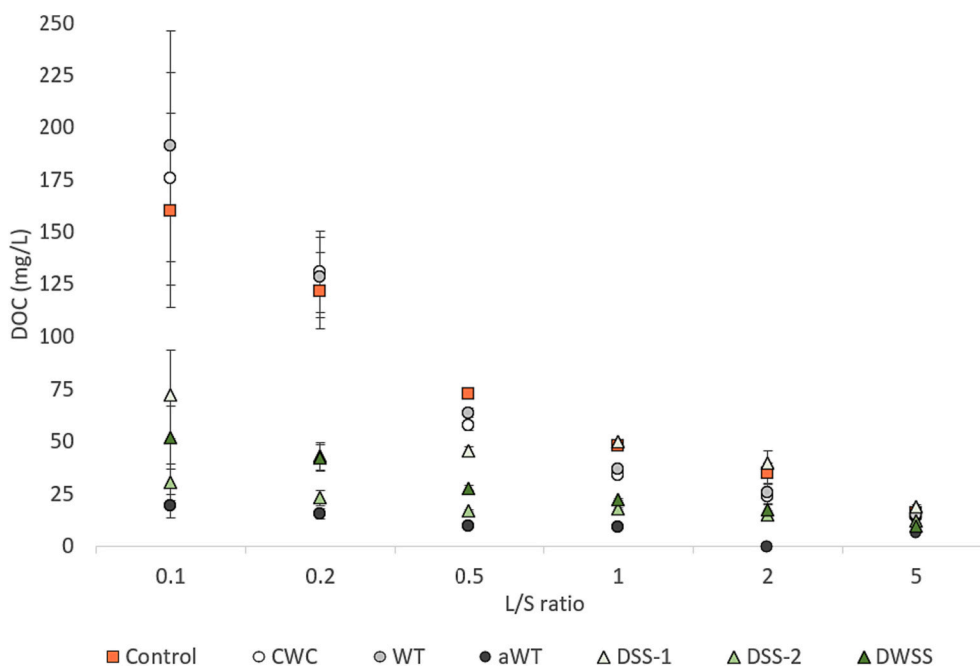


Fig. 4. Concentrations of dissolved organic carbon (DOC) [mg/L] in leachate samples from the unamended control column and the columns amended with clean wood chips (CWC), waste timber (WT), activated waste timber (aWT), digested sewage sludges (DSS-1 and DSS-2), and de-watered sewage sludge (DWSS) biochars (1 %). The x-axis is given as liquid to solid ratios (L/S). Error bars represent relative standard deviations based on partial measures of uncertainty.

**Table 3**

Attenuation factors (AF) [–] for PFAS sorption to biochar under influence of soil and a mixture of other PFAS. AFs were calculated using  $\log K_{d,BC-soil-mix}$  at L/S 0.1, and  $\log K_{d,BC-single}$  values both at the same water concentration ( $C_w$ , also shown in the table). Calculation of  $K_{d,BC-single}$  values, using  $\log K_{F,BC}$  from Krahn et al. (2023) of single PFAS-water batch tests at  $C_w$  of 1  $\mu\text{g/L}$ , were corrected to apply for the  $C_w$  detected at L/S 0.1. AFs differing less than a factor of 2 should not be considered statistically different (see text). AF-values below 2 should be considered as non-significant attenuation.

Biochar type		CWC				DSS-1				DWSS			
Compound	CF-chain length	$C_w$ [ $\mu\text{g/L}$ ]	$\log K_{d,BC-soil-mix}$	$\log K_{d,BC-single}$	AF	$C_w$ [ $\mu\text{g/L}$ ]	$\log K_{d,BC-soil-mix}$	$\log K_{d,BC-single}$	AF	$C_w$ [ $\mu\text{g/L}$ ]	$\log K_{d,BC-soil-mix}$	$\log K_{d,BC-single}$	AF
PFHxA	CF5	2.6	NA	NA	NA	1.0	NA	3.3	NA	1.7	2.9	4.7	52
PFHpA	CF6	0.3	NA	4.6	NA	0.1	1.8	5.1	1717	0.1	3.8	5.9	128
PFOA	CF7	1.3	0.3	5.0	53,690	0.3	2.8	5.3	316	0.2	3.9	6.0	114

surfaces (Fabregat-Palau et al., 2022). Attenuation factors (AF) for PFHxA, PFHpA and PFOA to the CWC, DSS-1 and DWSS biochars impacted by the presence of a mixture of at least 26 (quantifiable) PFAS as well as soil, are presented in Table 3. AFs for PFOA were far above one, indicating significant attenuation compared to the water-only, single-solute batch systems studied by Krahn et al. (2023). AFs decreased in the order: CWC (53690) > DSS-1 (316) > DWSS (114) for PFOA. The CWC biochar presented the strongest attenuation with AF of 53,690 for PFOA, indicating that sorption to this biochar was most strongly affected by sorption competition caused by presence of soil and/or other PFAS. Lower AF-values in the range of 52–128 and 316–1717 were observed for the DWSS and DSS-1 biochars respectively, indicating less competition for sorption in the wider pores in the sludge-based chars compared to those in the wood-based ones. The relatively low AFs for sludge biochars are in line with their observed strong PFAS sorption in the presence of soil and in an environmentally contaminated mixed-PFAS situation (Table 2). The standard deviations in the currently measured  $K_d$ -values and in the Krahn et al. (2023) values were both around 0.1–0.2 log units (Table 2). Thus, summarized standard deviations in AF-values were 0.2–0.3 log units, or 60–90 %. AFs differing less than a factor of 2 should thus not be considered statistically different. The relative differences between the CWC and sludge-based biochars can hence be considered significant.

The low TOC content of the unamended soil ( $0.57 \pm 0.04$  %, Table S.12) indicates that attenuation by competition for sorption sites with other PFAS probably exerted a stronger influence on overall sorption in the multisolute soil-biochar systems than pore blockage or competition for sorption sites with soil organic matter. This suggestion was also made by Krahn et al. (2023), based on their comparison of sorption attenuation to biochar in presence of 6 different PFAS with and without soil. In the present study, especially the very high PFOS concentration probably influenced the sorption of PFHxA, PFHpA and PFOA to the biochars.

### 3.6. Implications and limitations

Retardation factors for the untreated soil were around 5.0 (Table S17). Corresponding values for the most effective sludge biochar (DWSS) were around 400, and for aWT around 4000, i.e., 80 and 800 times higher than for untreated soil, respectively. This means for example that if 90 % of PFOS was leached from an untreated soil in 15 y, then 90 % leaching occurred after 1200 y for DWSS biochar-amended soil and after 12,000 y for aWT biochar-amended soil. Note that these are lower limit values as they assume that all biochar-sorbed PFOS desorbs at a rate equal to the PFOS desorbed in the first 2 weeks, where desorption rates may decrease over time due to PFOS in the deeper pores of the biochar being retained longer.

There are multiple studies in the literature demonstrating the remediation effect of carbonaceous sorbents on PFAS (see e.g., Navarro et al., 2023; Silvani et al., 2019; Sörensén et al., 2020; Sormo et al., 2021) based on simple laboratory batch tests. Data from ex situ and in situ studies of sorbent application in contaminated soils are necessary to

properly document the scalability and potential limitations of the concept. The present work has provided such data along with a measure of the attenuation one can expect when going from batch tests to column test. Meanwhile, the up flow column percolation tests are performed under saturated conditions. Additional attenuation of the sorbent effect is expected when the sorbents are applied in the unsaturated zone due to shorter contact times between sorbent and sorbate, and for longer-chain PFAS sorption to the air-water interface (Lyu and Brusseau, 2020). Hence, data from unsaturated column test or in situ field tests are still needed to fully understand the potential limitations of contaminated soil stabilization with carbonaceous sorbents.

Applying sorbents to contaminated soil, furthermore, comes with some practical challenges. Ex situ stabilization in landfill cells is likely the simplest approach, as soil and sorbents can be homogeneously mixed before disposal. Topsoil application through broadcasting and ploughing is a possible approach for in situ application and has been tested in connection with biochar for agricultural soil improvement (Cornelissen et al., 2018). This can be part of a treatment train, for instance through first performing local excavation for soil washing ex situ (Høisæter et al., 2021), followed by mixing with biochar before depositing at a landfill or the site of excavation. Recent technological advances have demonstrated the possibility of pressurised sorbent injection into the saturated soil layers of contaminated aquifers (Zhang et al., 2019). The creation of permeable reactive barriers perpendicular to groundwater flow has also been tried and tested for various reactive materials and contaminant combinations (Obiri-Nyarko et al., 2014).

Accumulation of metal(oid)s in sewage sludge biochars has been widely documented and can result in concentrations above thresholds established for fertilizer products and biochars for agricultural soil application (Agrafioti et al., 2013; Chanaka Udayanga et al., 2019; Kistler et al., 1987). The sewage sludge biochars (DSS-1, DSS-2 and DWSS) exceeded the European Biochar Certificate (EBC) agricultural use thresholds (EBC, 2012) for Cu and Zn (Table S.10). Elemental analysis of the column leachates (Table S.20 and Table S.21) demonstrated a net reduction in the leaching of potentially toxic heavy metals, such as As, Ba, Cr, Cu, Ni, V, and Zn, from soil amended with the sewage sludge biochars and a net release of nutrients such as K, Mg, and Na. However, net release of Cd (1.6  $\mu\text{g/kg}$  for DSS-1), Co (97  $\mu\text{g/kg}$  for DSS-1), Mo (56–121  $\mu\text{g/kg}$ ), and Pb (19 and 2.9  $\mu\text{g/kg}$  for DSS-1 and DWSS respectively) was also observed. The leaching of these metals from sewage sludge biochar upon application should be weighed against the positive contribution from the reduction of PFAS leaching. These data indicate that the overall risk of metal(oid) leaching from sewage sludge biochars could be low, although data representing long term in situ soil conditions are necessary to document the potential effect of soil weathering processes.

## 4. Conclusions and recommendations

This is the first study to demonstrate that field-collected soil samples, impacted with legacy PFAS contamination (i.e., not spiked), can be effectively stabilized by the application of waste/sludge-based biochars.

The results for the activated waste timber biochar (aWT) and the three sludge biochars were especially promising, as addition of only 1 % of these four biochars reduced the PFOS leaching from soil with >90 % compared to the unamended soil. Our experiments showed that there is a net retention of DOC by the sludge and activated biochars. Future work should determine the distribution of PFAS into the DOC and look at the DOC effect on retention and desorption of PFAS from biochar-amended soil systems. Novel insight could also be obtained by calculations on the importance of biochar surface charge for the adsorption of PFAS, shedding light on the relative contribution of electrostatic interactions and hydrophobic van de Waals interactions to the binding of short and long-chain PFAS.

Validation of the observations is recommended in the form of long-term field and laboratory trials, e.g., in bigger columns or under more realistic environmental conditions, such as lysimeters, as stronger reductions in long-term effectiveness have been predicted for biochar than for AC, due to lower overall capacities (Navarro et al., 2023). Since the results demonstrated lower effectiveness of the biochar amendments for more water-soluble and mobile short-chained PFAS, we recommend the importance of developing new techniques for the remediation of these compounds, such as novel materials or treated biochar sorbents (Aumeier et al., 2023).

The novel sludge-based sorbents effectively reduced leaching from a highly AFFF contaminated soil despite a certain degree of pore clogging by soil organic matter and sorptive competition between various PFAS compounds. We recommend verification in soils with higher TOC content and/or other PFAS contamination patterns.

Application of waste-based biochar sorbents for remediation of contaminated soil can have a positive impact on future waste management practices as this approach leads to a better embodiment of the waste reduction and reuse principles. For instance, sludge produced from AFFF-impacted wastewater can be converted into sludge biochar, which would remove the PFAS during pyrolysis, and result in a product that could be used to stabilize further PFAS emissions in the AFFF contaminated soil. Additional benefits also come in the form of carbon sequestration by placing these stable biochars in the soil. Further optimization of this approach is needed for short-chain PFAS, and to understand potential PFAS biproducts formed from various pyrolysis technologies.

#### CRedit authorship contribution statement

**Erlend Sørmo:** Writing – review & editing, Writing – original draft, Visualization, Validation, Supervision, Methodology, Investigation, Funding acquisition, Formal analysis, Data curation, Conceptualization. **Clara Benedikte Mader Lade:** Writing – original draft, Methodology, Investigation, Formal analysis. **Junjie Zhang:** Writing – review & editing, Methodology, Investigation, Data curation. **Alexandros G. Asimakopoulos:** Writing – review & editing, Supervision, Investigation, Data curation. **Geir Wold Åsli:** Methodology, Investigation. **Michel Hubert:** Writing – review & editing, Investigation, Data curation. **Aleksandar I. Goranov:** Investigation, Formal analysis. **Hans Peter H. Arp:** Writing – review & editing, Supervision, Funding acquisition. **Gerard Cornelissen:** Writing – review & editing, Writing – original draft, Validation, Supervision, Project administration, Investigation, Funding acquisition, Data curation, Conceptualization.

#### Declaration of competing interest

The authors declare that they have no known competing financial interests or personal relationships that could have appeared to influence the work reported in this paper.

#### Data availability

Data will be made available on request.

#### Acknowledgements

This work was funded by the Research Council of Norway, through the joint-industry sustainability (BIA-X) project “Valorization of Organic Waste” (VOW) (NFR 299070), the Miljøforsk project SLUDGEFFECT (NFR 302371) and the Horizon Europe project ARAGORN under grant agreement 101112723.

#### Appendix A. Supplementary data

Supplementary data to this article can be found online at <https://doi.org/10.1016/j.scitotenv.2024.170971>.

#### References

- Agrafioti, E., Bouras, G., Kalderis, D., Diamadopoulos, E., 2013. Biochar production by sewage sludge pyrolysis. *J. Anal. Appl. Pyrolysis* 101, 72–78. <https://doi.org/10.1016/j.jaap.2013.02.010>.
- Ahmad, M., Rajapaksha, A.U., Lim, J.E., Zhang, M., Bolan, N., Mohan, D., et al., 2014. Biochar as a sorbent for contaminant management in soil and water: a review. *Chemosphere* 99, 19–33. <https://doi.org/10.1016/j.chemosphere.2013.10.071>.
- Arvaniti, O.S., Asimakopoulos, A.G., Dasenaki, M.E., Ventouri, E.L., Stasinakis, A.S., Thomaidis, N.S., 2014. Simultaneous determination of eighteen perfluorinated compounds in dissolved and particulate phases of wastewater, and in sewage sludge by liquid chromatography–tandem mass spectrometry. *Anal. Methods* 6, 1341–1349.
- Asimakopoulos, A.G., Wang, L., Thomaidis, N.S., Kannan, K., 2014. A multi-class bioanalytical methodology for the determination of bisphenol a diglycidyl ethers, p-hydroxybenzoic acid esters, benzophenone-type ultraviolet filters, triclosan, and triclocarban in human urine by liquid chromatography–tandem mass spectrometry. *J. Chromatogr. A* 1324, 141–148.
- Aumeier, B.M., Georgi, A., Saeidi, N., Sigmund, G., 2023. Is sorption technology fit for the removal of persistent and mobile organic contaminants from water? *Sci. Total Environ.* 880, 163343.
- Bolan, N., Sarkar, B., Yan, Y., Li, Q., Wijesekera, H., Kannan, K., et al., 2021. Remediation of poly- and perfluoroalkyl substances (PFAS) contaminated soils – to mobilize or to immobilize or to degrade? *J. Hazard. Mater.* 401, 123892 <https://doi.org/10.1016/j.jhazmat.2020.123892>.
- Bostick, K.W., Zimmerman, A.R., Wozniak, A.S., Mitra, S., Hatcher, P.G., 2018. Production and composition of pyrogenic dissolved organic matter from a logical series of laboratory-generated chars. *Front. Earth Sci.* 6 <https://doi.org/10.3389/feart.2018.00043>.
- Buck, R.C., Franklin, J., Berger, U., Conder, J.M., Cousins, I.T., De Voogt, P., et al., 2011. Perfluoroalkyl and polyfluoroalkyl substances in the environment: terminology, classification, and origins. *Integr. Environ. Assess. Manag.* 7, 513–541. <https://doi.org/10.1002/ieam.258>.
- Chanaka Udayanga, W.D., Veksha, A., Giannis, A., Liang, Y.N., Lisak, G., Hu, X., Lim, T.-T., 2019. Insights into the speciation of heavy metals during pyrolysis of industrial sludge. *Sci. Total Environ.* 691, 232–242. <https://doi.org/10.1016/j.scitotenv.2019.07.095>.
- Cordner, A., Goldenman, G., Birnbaum, L.S., Brown, P., Miller, M.F., Mueller, R., et al., 2021. The true cost of PFAS and the benefits of acting now. *Environ. Sci. Technol.* 55, 9630–9633.
- Cornelissen, G., Gustafsson, Ö., 2006. Effects of added PAHs and precipitated humic acid coatings on phenanthrene sorption to environmental black carbon. *Environ. Pollut.* 141, 526–531. <https://doi.org/10.1016/j.envpol.2005.08.053>.
- Cornelissen, G., Jubaedah, Nurida, Hale, S.E., Martinsen, V., Silvani, L., Mulder, J., 2018. Fading positive effect of biochar on crop yield and soil acidity during five growth seasons in an Indonesian Ultisol. *Sci. Total Environ.* 634, 561–568. <https://doi.org/10.1016/j.scitotenv.2018.03.380>.
- Du, Z., Deng, S., Bei, Y., Huang, Q., Wang, B., Huang, J., et al., 2014. Adsorption behavior and mechanism of perfluorinated compounds on various adsorbents - a review. *J. Hazard. Mater.* 274, 443–454.
- EBC, 2012. European Biochar Certificate (No. Version 8.2E). European Biochar Foundation, Arbaz, Switzerland.
- EN 13137 (2001) Characterisation of waste. Determination of total organic carbon (TOC) in waste, sludges and sediments.
- EN 14405 (2017), Characterization of waste - leaching behaviour test - up-flow percolation test (under specified conditions).
- EN 1484 (1997). Water analysis. Guidelines for the determination of total organic carbon (TOC) and dissolved organic carbon (DOC).
- Eschazuer, C., Beerendonk, E., Scholte-Veenendaal, P., De Voogt, P., 2012. Impact of treatment processes on the removal of perfluoroalkyl acids from the drinking water production chain. *Environ. Sci. Technol.* 46, 1708–1715.
- Fabregat-Palau, J., Vidal, M., Rigol, A., 2022. Examining sorption of perfluoroalkyl substances (PFAS) in biochars and other carbon-rich materials. *Chemosphere* 302, 134733.
- Fenton, S.E., Ducatman, A., Boobis, A., DeWitt, J.C., Lau, C., Ng, C., Smith, J.S., Roberts, S.M., 2021. Per- and polyfluoroalkyl substance toxicity and human health review: Current state of knowledge and strategies for informing future research. In: *Environmental Toxicology and Chemistry*, Vol. 40. Wiley Blael, pp. 606–630. Issue 3.



- Goss, K.-U., Bronner, G., Harner, T., Hertel, M., Schmidt, T.C., 2006. The partition behavior of Fluorotelomer alcohols and olefins. *Environ. Sci. Technol.* 40, 3572–3577.
- Hale, S.E., Arp, H.P., Kupryianchik, D., Cornelissen, G., 2016. A synthesis of parameters related to the binding of neutral organic compounds to charcoal. *Chemosphere* 144, 65–74.
- Higgins, C.P., Luthy, R.G., 2006. Sorption of perfluorinated surfactants on sediments. *Environ. Sci. Technol.* 40, 7251–7256.
- Høisæter, Å., Breedveld, G.D., 2022. Leaching potential of per- and polyfluoroalkyl substances from source zones with historic contamination of aqueous film forming foam - a surfactant mixture problem. *Environ. Adv.* 8 <https://doi.org/10.1016/j.envadv.2022.100222>.
- Høisæter, Å., Pfaff, A., Breedveld, G.D., 2019. Leaching and transport of PFAS from aqueous film-forming foam (AFFF) in the unsaturated soil at a firefighting training facility under cold climatic conditions. *J. Contam. Hydrol.* 222, 112–122.
- Høisæter, Å., Arp, H.P.H., Slinde, G., Knutsen, H., Hale, S.E., Breedveld, G.D., Hansen, M. C., 2021. Excavated vs novel in situ soil washing as a remediation strategy for sandy soils impacted with per- and polyfluoroalkyl substances from aqueous film forming foams. *Sci. Total Environ.* 794, 148763.
- Hubert, M., Arp, H.P.H., Hansen, M.C., Castro, G., Meyn, T., Asimakopoulos, A.G., et al., 2023. Influence of grain size, organic carbon and organic matter residue content on the sorption of per- and polyfluoroalkyl substances in aqueous film forming foam contaminated soils-implications for remediation using soil washing. *Sci. Total Environ.* 875, 162668.
- Kissa, E., 2001. Physical and chemical properties. *Fluor. Surf. Repell.* 80–102.
- Kistler, R.C., Widmer, F., Brunner, P.H., 1987. Behavior of chromium, nickel, copper, zinc, cadmium, mercury, and lead during the pyrolysis of sewage sludge. *Environ. Sci. Technol.* 21, 704–708. <https://doi.org/10.1021/es00161a012>.
- Krafft, M.P., Riess, J.G., 2015. Per- and polyfluorinated substances (PFASs): environmental challenges. *Curr. Opin. Colloid Interface Sci.* 20, 192–212. <https://doi.org/10.1016/j.cocis.2015.07.004>.
- Krahn, K.M., Cornelissen, G., Castro, G., Arp, H.P.H., Asimakopoulos, A.G., Wolf, R., et al., 2023. Sewage sludge biochars as effective PFAS-sorbents. *J. Hazard. Mater.* 445, 130449.
- Kupryianchik, D., Hale, S., Zimmerman, A.R., Harvey, O., Rutherford, D., Abiven, S., et al., 2016a. Sorption of hydrophobic organic compounds to a diverse suite of carbonaceous materials with emphasis on biochar. *Chemosphere* 144, 879–887.
- Kupryianchik, D., Hale, S.E., Breedveld, G.D., Cornelissen, G., 2016b. Treatment of sites contaminated with perfluorinated compounds using biochar amendment. *Chemosphere* 142, 35–40. <https://doi.org/10.1016/j.chemosphere.2015.04.085>.
- Liu, Z., Zhang, P., Wei, Z., Xiao, F., Liu, S., Guo, H., Qu, C., Xiong, J., Sun, H., Tan, W., 2023. Porous Fe-doped graphitized biochar: an innovative approach for co-removing per-/polyfluoroalkyl substances with different chain lengths from natural waters and wastewater. *Chem. Eng. J.* 476, 146888 <https://doi.org/10.1016/j.cej.2023.146888>.
- Lyu, Y., Brusseau, M.L., 2020. The influence of solution chemistry on air-water interfacial adsorption and transport of PFOA in unsaturated porous media. *Sci. Total Environ.* 713, 136744.
- Mahinroosta, R., Senevirathna, L., 2020. A review of the emerging treatment technologies for PFAS contaminated soils. *J. Environ. Manag.* 255 <https://doi.org/10.1016/j.jenvman.2019.109896>.
- Navarro, D.A., Kabiri, S., Ho, J., Bowles, K.C., Davis, G., McLaughlin, M.J., et al., 2023. Stabilisation of PFAS in soils: long-term effectiveness of carbon-based soil amendments. *Environ. Pollut.* 323, 121249.
- Nelson, D.W., Sommers, L.E., 1983. Total carbon, organic carbon, and organic matter. *Method Soil Anal.* 539–579.
- Nguyen, T.M.H., Bräunig, J., Thompson, K., Thompson, J., Kabiri, S., Navarro, D.A., et al., 2020. Influences of chemical properties, soil properties, and solution pH on soil-water partitioning coefficients of per- and polyfluoroalkyl substances (PFASs). *Environ. Sci. Technol.* 54, 15883–15892.
- Obiri-Nyarko, F., Grajales-Mesa, S.J., Malina, G., 2014. An overview of permeable reactive barriers for in situ sustainable groundwater remediation. *Chemosphere* 111, 243–259. <https://doi.org/10.1016/j.chemosphere.2014.03.112>.
- Pignatello, J., Mitch, W.A., Xu, W., 2017. Activity and reactivity of pyrogenic carbonaceous matter toward organic compounds. *Environ. Sci. Technol.* 51, 8893–8908.
- Quinnan, J., Morrell, C., Nagle, N., Maynard, K.G., 2022. Ex situ soil washing to remove PFAS adsorbed to soils from source zones. *Remediat. J.* 32, 151–166.
- Rayne, S., Forest, K., 2016. Estimated pK<sub>a</sub> values for the environmentally relevant C1 through C8 perfluorinated sulfonic acid isomers. *J. Environ. Sci. Health A* 51, 1018–1023.
- Ross, I., McDonough, J., Miles, J., Storch, P., Thelakkat Kochunarayanan, P., Kalve, E., et al., 2018. A review of emerging technologies for remediation of PFASs. *Remediat. J.* 28, 101–126. <https://doi.org/10.1002/rem.21553>.
- Ruyle, B.J., Thackray, C.P., Butt, C.M., Leblanc, D.R., Tokranov, A.K., Vecitis, C.D., et al., 2023. Centennial persistence of forever Chemicals at Military Fire Training Sites. *Environ. Sci. Technol.* 57, 8096–8106.
- Sigmund, G., Arp, H.P.H., Aumeier, B.M., Bucheli, T.D., Chefetz, B., Chen, W., et al., 2022. Sorption and mobility of charged organic compounds: how to confront and overcome limitations in their assessment. *Environ. Sci. Technol.* 56, 4702–4710.
- Silvani, L., Cornelissen, G., Smebye, A.B., Zhang, Y.X., Okkenhaug, G., Zimmerman, A.R., et al., 2019. Can biochar and designer biochar be used to remediate per- and polyfluorinated alkyl substances (PFAS) and lead and antimony contaminated soils? *Sci. Total Environ.* 694 <https://doi.org/10.1016/j.scitotenv.2019.133693>.
- Smebye, A., Alling, V., Vogt, R.D., Gadmar, T.C., Mulder, J., Cornelissen, G., et al., 2016. Biochar amendment to soil changes dissolved organic matter content and composition. *Chemosphere* 142, 100–105.
- Söregård, M., Kleja, D.B., Ahrens, L., 2019a. Stabilization of per- and polyfluoroalkyl substances (PFASs) with colloidal activated carbon (PlumeStop (R)) as a function of soil clay and organic matter content. *J. Environ. Manag.* 249, 7. <https://doi.org/10.1016/j.jenvman.2019.109345>.
- Söregård, M., Kleja, D.B., Ahrens, L., 2019b. Stabilization and solidification remediation of soil contaminated with poly- and perfluoroalkyl substances (PFASs). *J. Hazard. Mater.* 367, 639–646. <https://doi.org/10.1016/j.jhazmat.2019.01.005>.
- Söregård, M., Ostblom, E., Kohler, S., Ahrens, L., 2020. Adsorption behavior of per- and polyfluoroalkyl substances (PFASs) to 44 inorganic and organic sorbents and use of dyes as proxies for PFAS sorption. *J. Environ. Chem. Eng.* 8, 8. <https://doi.org/10.1016/j.jece.2020.103744>.
- Sørmo, E., Silvani, L., Bjerkli, N., Hagemann, N., Zimmerman, A.R., Hale, S.E., et al., 2021. Stabilization of PFAS-contaminated soil with activated biochar. *Sci. Total Environ.* 763 <https://doi.org/10.1016/j.scitotenv.2020.144034>.
- Sørmo, E., Castro, G., Hubert, M., Licul-Kucera, V., Quintanilla, M., Asimakopoulos, A.G., et al., 2023. The decomposition and emission factors of a wide range of PFAS in diverse, contaminated organic waste fractions undergoing dry pyrolysis. *J. Hazard. Mater.* 454, 131447.
- Sparrevik, M., Saloranta, T., Cornelissen, G., Eek, E., Fet, A.M., Breedveld, G.D., et al., 2011. Use of life cycle assessments to evaluate the environmental footprint of contaminated sediment remediation. *Environ. Sci. Technol.* 45, 4235–4241. <https://doi.org/10.1021/es103925u>.
- Tang, J., Cao, C., Gao, F., Wang, W., 2019. Effects of biochar amendment on the availability of trace elements and the properties of dissolved organic matter in contaminated soils. *Environ. Technol. Innov.* 16 <https://doi.org/10.1016/j.eti.2019.100492>.
- Thies, J.E., Rillig, M.C., 2009. Characteristics of biochar: Biological properties. In: Lehmann, J., Joseph, S. (Eds.), *Biochar for Environmental Management: Science and Technology*. Earthscan, pp. 85–106.
- Travari, U., Uwayezu, J.N., Kumpiene, J., Yeung, L.W.Y., 2020. Challenges in the PFAS remediation of soil and landfill leachate: a review. *Adv. Environ. Eng. Res.* 02, 1–40.
- Van der Sloot, H.A., Piepers, O., Kok, A., 1984. A Standard Leaching Test for Combustion Residues, Netherlands. Available on A standard leaching test for combustion residues (Book) | ETDEWEB. [osti.gov](https://doi.org/10.1021/es103925u).
- Vierke, L., Berger, U., Cousins, I.T., 2013. Estimation of the acid dissociation constant of perfluoroalkyl carboxylic acids through an experimental investigation of their water-to-air transport. *Environ. Sci. Technol.* 47, 11032–11039.
- Wagner, S., Brandes, J., Goranov, A.I., Drake, T.W., Spencer, R.G.M., Stubbs, A., 2017. Online quantification and compound-specific stable isotopic analysis of black carbon in environmental matrices via liquid chromatography-isotope ratio mass spectrometry. *Limnol. Oceanogr. Methods* 15, 995–1006. <https://doi.org/10.1002/lom3.10219>.
- Werner, D., Ghosh, U., Luthy, R.G., 2006. Modeling polychlorinated biphenyl mass transfer after amendment of contaminated sediment with activated carbon. *Environ. Sci. Technol.* 40, 4211–4218. <https://doi.org/10.1021/es052215k>.
- Wiedemeier, D.B., Abiven, S., Hockaday, W.C., Keiluweit, M., Kleber, M., Masiello, C.A., et al., 2015. Aromaticity and degree of aromatic condensation of char. *Org. Geochem.* 78, 135–143.
- Xiao, X., Ulrich, B.A., Chen, B., Higgins, C.P., 2017. Sorption of poly- and perfluoroalkyl substances (PFASs) relevant to aqueous film-forming foam (AFFF)-impacted groundwater by biochars and activated carbon. *Environ. Sci. Technol.* 51, 6342–6351.
- Zahm, S., Bonde, J.P., Chiu, W.A., Hoppin, J., Kanno, J., Abdallah, M., Blystone, C.R., Calkins, M.M., Dong, G.-H., Dorman, D.C., Fry, R., Guo, H., Haug, L.S., Hofmann, J. N., Iwasaki, M., Machala, M., Mancini, F.R., Maria-Engler, S.S., Møller, P., Schubauer-Berigan, M.K., 2023. Carcinogenicity of perfluorooctanoic acid and perfluorooctanesulfonic acid. *Lancet Oncol.* 25, 16–17.
- Zhang, W., Liang, Y., 2022. Performance of different sorbents toward stabilizing per- and polyfluoroalkyl substances (PFAS) in soil. *Environ. Adv.* 8 <https://doi.org/10.1016/j.envadv.2022.100217>.
- Zhang, C., Yan, H., Li, F., Hu, X., Zhou, Q., 2013. Sorption of short- and long-chain perfluoroalkyl surfactants on sewage sludges. *J. Hazard. Mater.* 260, 689–699. <https://doi.org/10.1016/j.jhazmat.2013.06.022>.
- Zhang, T., Lowry, G.V., Caprio, N.L., Chen, J., Chen, W., Chen, Y., Dionysiou, D.D., Elliott, D.W., Ghoshal, S., Hofmann, T., Hsu-Kim, H., Hughes, J., Jiang, C., Jiang, G., Jing, C., Kavanaugh, M., Li, Q., Liu, S., Ma, J., Pan, B., Pherrat, T., Qu, X., Quan, X., Saleh, N., Vikesland, P.J., Wang, Q., Westerhoff, P., Wong, M.S., Xia, T., Xing, B., Yan, B., Zhang, L., Zhou, D., Alvarez, P.J.J., 2019. In situ remediation of subsurface contamination: opportunities and challenges for nanotechnology and advanced materials. *Environ. Sci. Nano* 6, 1283–1302. <https://doi.org/10.1039/C9EN00143C>.
- Zhang, D., He, Q., Wang, M., Zhang, W., Liang, Y., 2021. Sorption of perfluoroalkylated substances (PFASs) onto granular activated carbon and biochar. *Environ. Technol.* 42, 1798–1809.
- Zimmerman, A.R., Goyné, K.W., Chorover, J., Komarneni, S., Brantley, S.L., 2004. Mineral mesopore effects on nitrogenous organic matter adsorption. *Org. Geochem.* 35, 355–375. <https://doi.org/10.1016/j.orggeochem.2003.10.009>.